Osteoprotegerin: a double-edged sword in osteoarthritis development

Rodriguez Ruiz, A.

CHAPTER 2

The role of *TNFRSF11B* in development of osteoarthritic cartilage

Alejandro Rodríguez Ruiz[1], Margo Tuerlings[1], Ankita Das[1], Rodrigo Coutinho de Almeida[1], H. Eka Suchiman[1], Rob GHH Nelissen[2], Yolande FM Ramos[1§*], and Ingrid Meulenbelt[1§]

[1]Department of Biomedical Data Sciences, Section Molecular Epidemiology and [2]Department of Orthopaedics, Leiden University Medical Center, Leiden, The Netherlands

Rheumatology (Oxford). 2022 Feb; 61(2): 856–864.

ABSTRACT

Objectives: Osteoarthritis (OA) is a complex genetic disease with different risk factors contributing to its development. One of the genes, *TNFRSF11B*, previously identified with gain-of-function mutation in a family with early-onset OA with chondrocalcinosis, is among the highest upregulated genes in lesioned OA cartilage (RAAK-study). Here, we determined the role of *TNFRSF11B* overexpression in development of OA.

Methods: Human primary articular chondrocytes (9 donors RAAK study) were transduced using lentiviral particles with or without *TNFRSF11B*. Cells were cultured for 1 week in a 3D *in-vitro* chondrogenic model . *TNFRSF11B* overexpression was confirmed by RT-qPCR, immunohistochemistry and ELISA. Effects of *TNFRSF11B* overexpression on cartilage matrix deposition, matrix mineralization, and genes highly correlated to *TNFRSF11B* in RNA-sequencing dataset (r>|0.75|) were determined by RT-qPCR. Additionally, glycosaminoglycans and collagen deposition were visualized with Alcian blue staining and immunohistochemistry (COL1 and COL2).

Results: Overexpression of *TNFRSF11B* resulted in strong upregulation of *MMP13*, *COL2A1* and *COL1A1*. Likewise, mineralization and osteoblast characteristic markers *RUNX2*, *ASPN* and *OGN* showed a consistent increase. Among 30 genes highly correlated to *TNFRSF11B*, expression of only eight changed significantly, with *BMP6* showing highest increase (9-fold) while expression of RANK and RANKL remained unchanged indicating previously unknown downstream pathways of *TNFRSF11B* in cartilage.

Conclusion: Results of our 3D *in vitro* chondrogenesis model indicate that upregulation of *TNFRSF11B* in lesioned OA cartilage may act as a direct driving factor for chondrocyte to osteoblast transition observed in OA pathophysiology. This transition does not appear to act via the OPG/RANK/RANKL triad common in bone remodeling.

Key messages:

- *TNFRSF11B* in cartilage is a direct driving factor for chondrocyte-to-osteoblast transition observed in OA pathophysiology.
- Chondrocyte-to-osteoblast transition in cartilage does not act via the OPG/RANK/RANKL triad, common in bone remodeling.
- Likely, the *TNFRSF11B*-induced cartilage mineralization is accomplished via BMP6 signaling.

INTRODUCTION

Osteoarthritis (OA) is a common degenerative disorder characterized by cartilage extracellular matrix degradation (ECM) and changes in subchondral bone. Being marked by pain and disability, no effective therapy is available, and current treatments are focused on pain relief or joint surgery at end-stage disease, creating a great social and economic burden (1, 2). To characterize the OA pathophysiological process, multiple studies (3-5) have performed transcriptome-wide analyses of preserved and lesioned cartilage. Among the most consistent and highly upregulated genes in lesioned OA cartilage is the tumor necrosis factor receptor superfamily member 11b (*TNFRSF11B*) at the CCAL1 (chondrocalcinosis) locus (4, 6), encoding osteoprotegerin (OPG). OPG is a decoy receptor for the binding of nuclear factor KB ligand (RANKL) to the receptor activator of the nuclear KB factor (RANK). Together, this triad is well known for tightly regulating osteoclastogenesis, hence playing a critical role in bone formation, endochondral ossification, and bone remodelling (5, 6). A gain of function mutation in OPG (c1205A=>T; p.Stop402Leu) was identified in multiple families with early onset osteoarthritis (FOA) characterized by chondrocalcinosis (6, 7). With this mutation, the underlying importance of OPG was further confirmed, not only in bone turnover but also in cartilage homeostasis and OA onset. Given the eminent cross-talk between bone and cartilage, it was suggested that aberrant OPG function can affect the delicate balance between subchondral bone formation and resorption (8), making OPG essential in joint homeostasis. A drug called strontium ranelate has been administered in the clinic in order to fight osteoporosis by increasing OPG expression and impairing bone resorption processes (9). This drug is also used to treat OA, but controversial results have been shown in preclinical and clinical studies (10, 11). To study whether the observed upregulation of *TNFRSF11B* in OA can trigger unbeneficial mineralization of cartilage, a tailored human 3D *in vitro* OA tissue model was applied in which aberrant gene function was mimicked by lentiviral overexpression of *TNFRSF11B* in spherical cartilage pellets. Potential effects on anabolic, catabolic and mineralization markers involved in cartilage homeostasis were investigated. Moreover, to better comprehend the pathways in which *TNFRSF11B* acts in articular cartilage and during OA, a selected panel of genes that showed high co-expression with *TNFRSF11B* during OA pathophysiology was studied.

MATERIALS AND METHODS

Sample description

RNA sequencing data previously obtained of N=57 preserved and N=44 lesioned OA cartilage samples (RAAK study) and previously assessed (4), were taken for *in silico TNFRSF11B* correlation analyses. RNA sequencing was used to identify genes

co-expressed with *TNFRSF11B,* where a Spearman correlation was performed. Genes were considered to be correlated if the P-value was lower than 0.05 and the absolute r-value was higher than 0.75. Quality control of the data was performed as previously described (4). Human primary articular chondrocytes (hPACs) obtained from knee replacement surgeries of N=9 participants (4 females and 5 males with average age of 69.4±11.1) of the RAAK study were isolated and cultured to perform lentiviral transduction.

Cloning of TNFRSF11B in lentivirus plasmid

The Porf9-H*TNFRSF11B* V04 plasmid and the pLV.CMV.bc.eGFP lentivirus vector (kindly provided by Prof. Dr. R. Hoeben) were digested with AgeI and NheI (New England Biolabs). The full gene *TNFRSF11B* was ligated into the AgeI and NheI sites of the K4_pLV.CMV.bc.eGFP plasmid by using the Takara Mighty Mix ligation kit (Takara Bio Europe AB). DNA was obtained by Maxiprep Kit (ThermoFisher), and Sanger sequencing was performed to confirm successful cloning of the lentivirus plasmid.

Lentiviral production and cell culture

Lentiviral production was performed in HEK293T cells using the Lenti-vpak Lentiviral Packaging Kit (Origene Technologies). In short, HEK 293T cells were expanded in DMEM high glucose (Gibco), supplemented with 10% fetal calf serum (FCS, Gibco) 100U/mL penicillin, 100ug/ml streptomycin (Gibco), and lentivirus particles were collected and titrated.

Following their isolation, hPACs were transduced at passage 1 with either control (pLV.CMV.bc.eGFP) or *TNFRSF11B* Lentivirus (MOI of 1). After 16 hours, the medium was refreshed (DMEM high glucose (Gibco) supplemented with 10% FCS (Gibco), 100 U/ml penicillin and 100 ug/ml streptomycin (Gibco), and 0.5 ng/ml bFGF-2 (PeproTech)) and hPACs were further cultured for another passage. Subsequently, neo-cartilage was generated from 250,000 transduced hPACs in 3D pellets for seven days, as described before (12), and keeping the conditions between both groups equal. All data were analyzed 7 days following the 3D chondrogenesis. Cells were counted with the Nucleocounter NC-200 (Chemometec).

RNA isolation and RT-qPCR

RNA was isolated from four biological replicates for each patient and condition (control and *TNFRSF11B*-overexpressing chondrocytes) while pooling two pellets together to generate two independent samples for downstream analyses. Isolations were performed as described previously (12). Total mRNA (150 ng) was processed with the first strand cDNA kit according to the manufacturer's protocol (Roche Applied Science). CDNA was further diluted five times, and preamplification with

TaqMan preamp master mix (Thermo Fisher Scientific Inc.) was performed. Gene expression was measured (**Supplementary Table S1**) with RT-qPCR (Quantstudio), and average of the two biological replicates was determined as relative levels (–ΔCt values) using expression levels of glyceraldehyde 3-phosphate dehydrogenase (*GAPDH*) and Acidic ribosomal phosphoprotein P0 (*ARP*) as housekeeping genes. Quality control of the results was performed as described before (12).

Selection criteria for gene expression analyses

TNFRSF11B expression was analyzed to quantify overexpression. To determine matrix homeostasis, metabolic activity and mineralization status, a list of 16 relevant genes was selected from the literature (**Supplementary Table S1**). Additionally, to identify potential new downstream pathways, a two-step approach was taken for selection of genes. Firstly, a *TNFRSF11B* co-expression network was created based on correlations of genes significantly differentially expressed between preserved (N = 57) and lesioned (N = 44) OA cartilage from our previously published RNA sequencing dataset (N=2387 genes) (4). Genes with $r \geq |0.80|$ were selected for expression analysis (N=21 genes). Secondly, genes with $r > |0.75|$ were designated on basis of their functionality in cartilage homeostasis and mineralization (6 genes), or based on previously identified protein-protein interactions with *TNFRSF11B* within the online available webtool STRING (13) (three genes). This resulted in a total of 30 genes. Finally, *GAPDH* and *ARP* were used as housekeeping genes.

Histology and immunohistochemistry

Following chondrogenesis, pellets were fixed in 4% formaldehyde and embedded in paraffin. After sectioning, deparaffinization and rehydration sections were analyzed by histology (1% Alcian Blue 8-GX (Sigma-Aldrich)) and immunohistochemistry (COL2 (MAB1330; Milipore; 1:100), COL1 (ab34710; Abcam), and OPG (EPR3592; Epitomics; 1:100)), as described before (12). Pixel intensity quantification was performed for Alcian Blue staining by ImageJ, and surface area of the pellets were measured with the CellSens Dimension software (Olympus).

ELISA and DMMB assay

The osteoprotegerin human instant ELISA™ Kit (Thermofisher) and the Dimethylmethylene Blue assay (DMMB; Sigma-Aldrich), respectively, were used following the manufacturer's instructions for OPG and GAG quantification in the conditioned media of three independent pellets with or without *TNFRSF11B* overexpression for each patient.

Statistical analysis

To determine statistical differences between the controls and samples with *TNFRSF11B* overexpression, a paired sample t-test was performed. P-value <0.05 was considered significant.

RESULTS

No change in matrix deposition upon TNFRSF11B overexpression

Lentiviral transduction of primary chondrocytes resulted in consistent and significant upregulation of *TNFRSF11B* mRNA as well as OPG protein (**Supplementary Figure S1**). Following *TNFRSF11B* overexpression, hPACs were subjected to a 3D *in vitro* chondrogenesis model, and neo-cartilage formation was characterized at day seven.

Alcian Blue staining was performed to visualize pellets and the presence of glycosaminoglycans (GAGs). The relative pixel intensity of the GAG staining showed no significant differences in the presence of higher OPG levels (n=18, P-value=$3.4x10^{-1}$; **Figure 1**). Likewise, GAG release in the medium was similar (n=27, P-value=$5.3x10^{-1}$). Furthermore, no significant difference in pellet size was observed between controls and *TNFRSF11B* (n=72, P-value=$5.5x10^{-1}$). Together, these data indicate that *TNFRSF11B* upregulation does not change capacity of chondrocytes to deposit matrix at day 7.

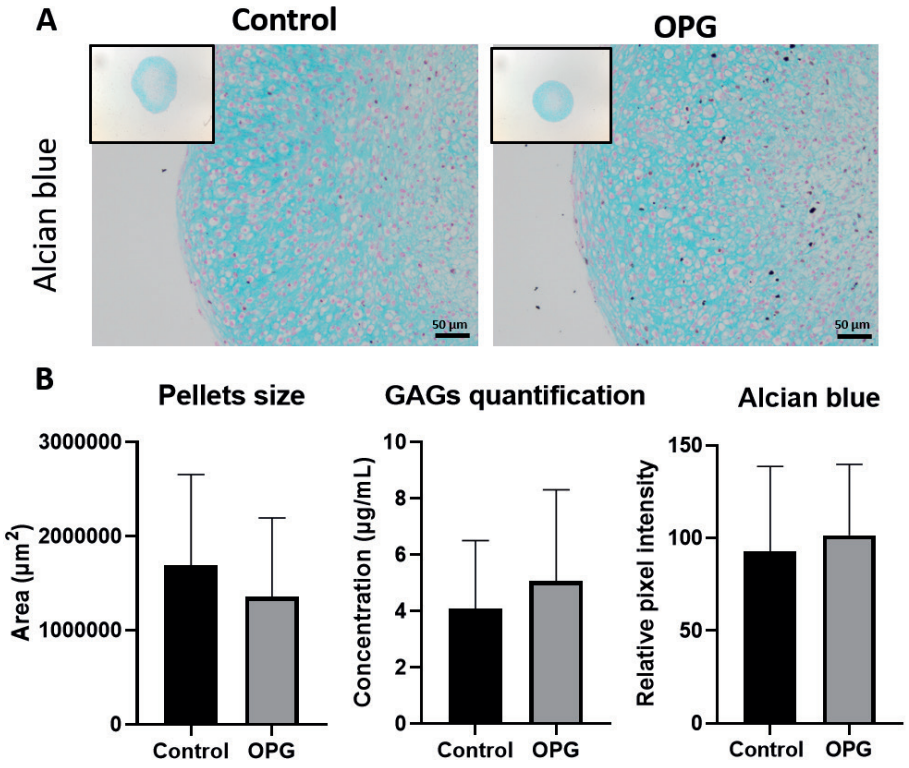

Figure 1. Neo-cartilage deposition upon *TNFRSF11B* overexpression. A) Representative images of 1-week neo-cartilage pellets as indicated (left: control chondrocytes; right: chondrocytes with *TNFRSF11B* overexpression). Scale bars: 50 µm. **B)** Area of the pellets (n=72), GAG-release in the medium (n=27), and Alcian blue pixel intensity quantification (n=18) for control and *TNFRSF11B* overexpressing chondrocytes.

Collagen type I and collagen type II become upregulated upon TNFRSF11B overexpression

To study the effect of *TNFRSF11B* overexpression on matrix characteristics, RT-qPCR was performed for anabolic and catabolic genes involved in cartilage homeostasis (**Supplementary Table S2, Figure 2**). Of note was the high and significant upregulation of *MMP13* (FD=14.76, P-value=2.0x10^{-3}) following overexpression of *TNFRSF11B* (**Figure 2**). Furthermore, overexpression of *TNFRSF11B* resulted in significantly higher upregulation of *COL2A1* (FD=4.77, P-value=4.8x10^{-4}) and *COL1A1* (FD=1.88, P-value=1.3x10^{-2}) and a modest downregulation of *COMP* (FD=0.69, P-value=2.0x10^{-2}) during chondrogenesis. Hypertrophic marker *COL10A1* showed no significant difference (FD=4.24, P-value=6.3x10^{-1}). Immunohistochemistry of collagen type 2 (COL2) and collagen type 1 (COL1) showed a visual higher expression for both collagens in the OPG overexpressing group concurrent with respective gene expression levels (**Figure 3**). As such, COL1 staining showed a

darker and wider layer of staining towards the edges of the pellet when compared to the control group. COL2 differences were less strong between both conditions, nevertheless a more consistent staining was observed in the ECM and retained within the cells cytoplasm in the OPG overexpressing group.

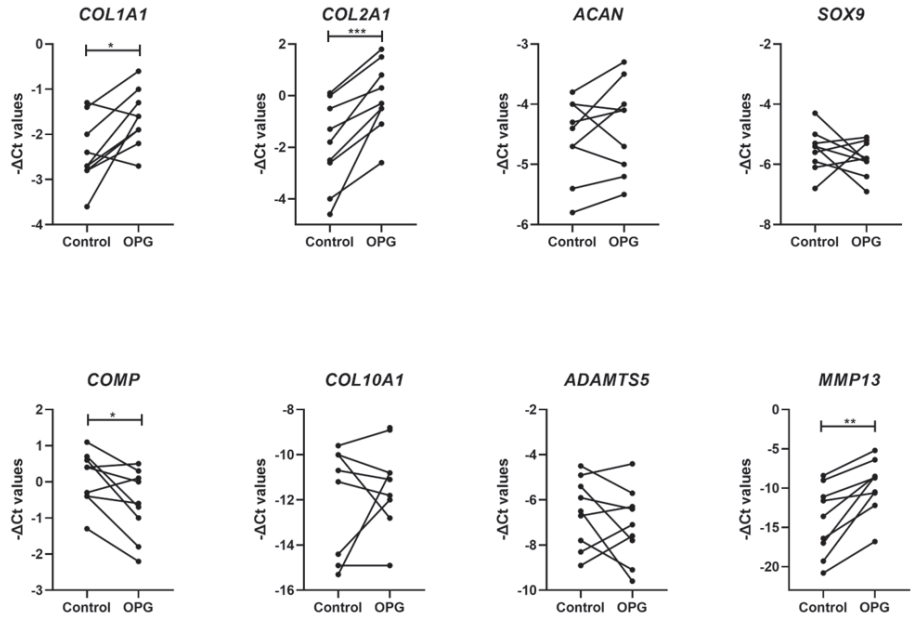

Figure 2. Expression of matrix-related genes in neo-cartilage. Results show line plots for -ΔCt values of genes in 1-week neo-cartilage pellets (control chondrocytes versus chondrocytes with *TNFRSF11B* overexpression (n=18; * P-value< 0.05; ** P-value< 10^{-3}; *** P-value< 10^{-6}).

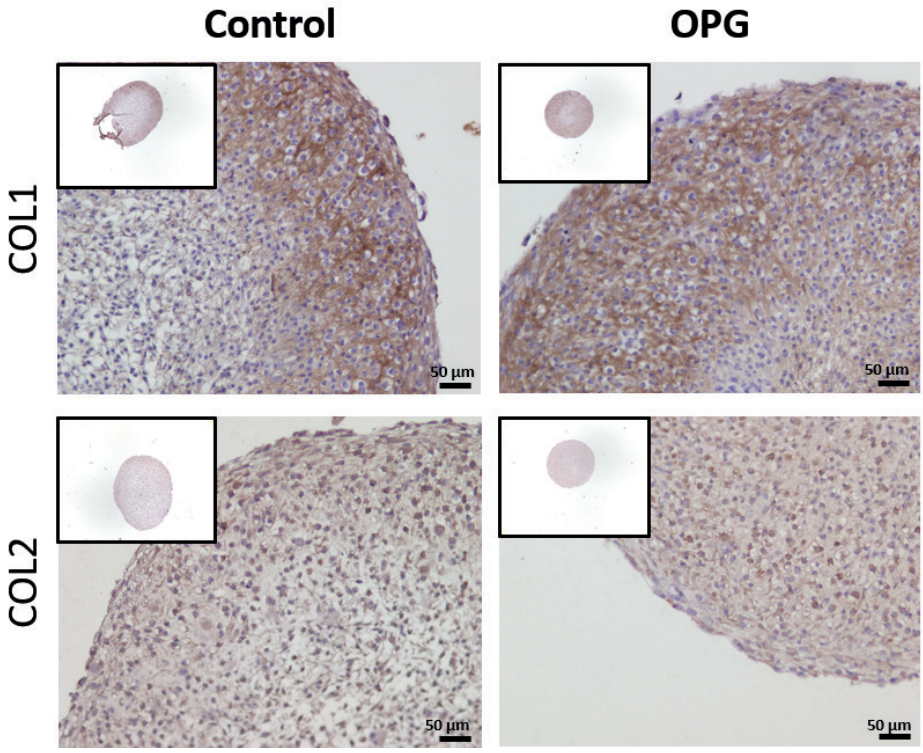

Figure 3. COL1 and COL2 immunohistochemistry of neo-cartilage. Representative images of 1-week neo-cartilage pellets as indicated (left: control chondrocytes; right: chondrocytes with *TNFRSF11B* overexpression). Scale bars: 50µm.

High gene expression of osteogenic markers, yet no alteration in the TNFRSF11B triad upon TNFRSF11B overexpression

To investigate our hypothesis that upregulation of *TNFRSF11B* with OA pathophysiology directly induces cartilage mineralization, we next explored the expression of genes involved in matrix mineralization (**Supplementary table S2**). First, we explored expression of *TNFRSF11A* encoding RANK and *TNFSF11* encoding RANKL, which together with OPG are known to tightly regulate bone turnover. Remarkably (**Figure 4**), neither *TNFSF11* (FD=1.06, P-value=3.9x10^{-1}) nor *TNFRSF11A* (FD=2.45, P-value=7.8x10^{-1}), did significantly respond to the lentiviral-induced upregulation of *TNFRSF11B*. Nonetheless, the osteogenic markers *RUNX2* (FD=4.51, P-value=4.0x10^{-3}), *POSTN* (FD=1.75, P-value=4.0x10^{-2}), *OGN* (FD=1.68, P-value=2.3x10^{-2}) and *ASPN* (FD=2.61, P-value=1.0x10^{-2}), were significantly higher upregulated in chondrocytes upon *TNFRSF11B* overexpression.

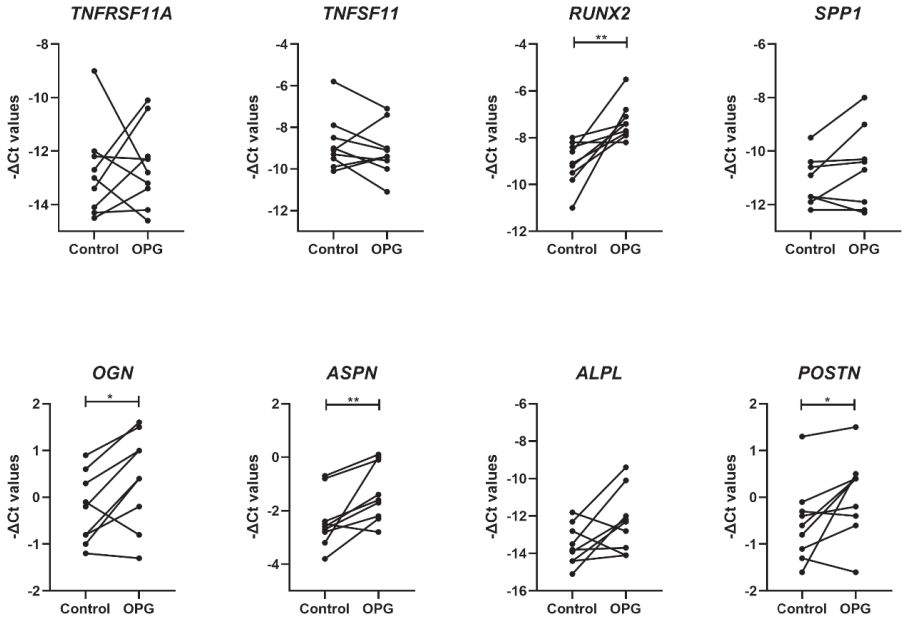

Figure 4. Expression of osteogenic-related genes in neo-cartilage. Results show line plots for -ΔCt values of mineralization and bone formation genes in 1-week neo-cartilage pellets (control chondrocytes versus chondrocytes with *TNFRSF11B* overexpression (n=18; * P-value< 0.05; ** P-value< 10^{-3} ;*** P-value< 10^{-6}).

A novel set of signaling pathways is discovered in highly correlated genes with TNFRSF11B upon TNFRSF11B overexpression

After assessing the effect of *TNFRSF11B*-induced overexpression on known related genes, we next performed an exploratory analysis to identify potential novel *TNFRSF11B* signaling pathways in cartilage. To do so, we generated a *TNFRSF11B* co-expression network with differentially expressed genes between preserved and lesioned OA cartilage as previously assessed (N=2387 genes) (4). We found 51 genes highly correlated with *TNFRSF11B* with absolute r-values ≥ 0.75 (**Supplementary Table S3**). Among the highest positively correlated genes, we found *CDH19* (r=0.88), *ATP1A1* (r=0.87), and *DIXDC1* (r=0.85), whereas the highest inverse correlation was observed for *SLC15A3* (r=-0.81), *MAPK11* (r=-0.81), and *HLA-E* (r=-0.8). Of these 51 genes, 30 were selected for expression analysis based on their correlation with *TNFRSF11B* and additional functional connection in STRING (**Supplementary Figure S2**). As shown in **Supplementary Table S4** and **Figure 5**, we found eight genes to be significantly differentially expressed upon lentiviral-induced *TNFRSF11B* overexpression. The strongest increased expression was found for *BMP6* (FD=9.34, P-value=$2.6x10^{-2}$) while the *SLC15A3* gene was 2.5-fold downregulated (FD=0.4, P-value=$4.0x10^{-3}$). Around

2-fold increase was observed for *FITM2* (FD=2.28, P-value=1.4x10^{-2}), *CDON* (FD=2.03, P-value=5.0x10^{-3}), and *SLC16A7* (FD=1.97, P-value=1.8x10^{-2}). Moderate effects were found for *CDH19* (FD=1.53, P-value=4.5x10^{-2}), *P3H2* (FD=1.48, P-value=4.7x10^{-2}), and *WNT16* (FD=0.81, P-value=4.3x10^{-2}).

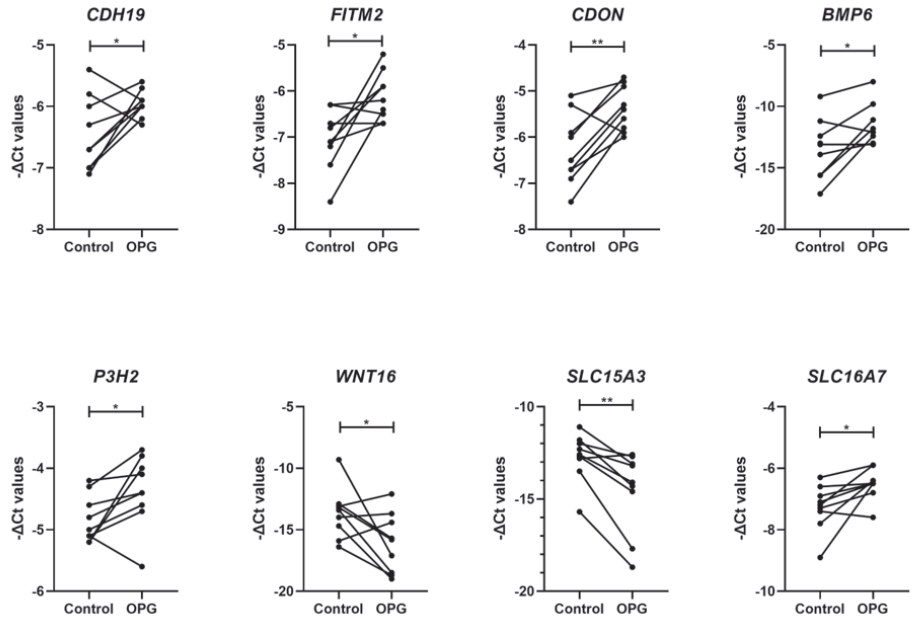

Figure 5. Expression of *TNFRSF11B*-correlated genes in neo-cartilage. Results show line plots for -ΔCt values of *TNFRSF11B*-correlated genes in 1-week neo-cartilage pellets (control chondrocytes versus chondrocytes with *TNFRSF11B* overexpression (n=18; * P-value< 0.05; ** P-value< 10^{-3}; *** P-value< 10^{-6}).

DISCUSSION

In the current study, we investigated the role of increased *TNFRSF11B* in OA pathophysiology. To this end, lentiviral upregulation of *TNFRSF11B* was established in a 3D *in vitro* chondrogenic model (**Supplementary Figure S1**). As reflected by the particularly high upregulation of *MMP13* (FD=14.76, P-value=2.0x10^{-3}) in combination with the upregulation of characteristic osteogenic genes *RUNX2, POSTN, BMP6, ASPN,* and *OGN* and in absence of differential expression of the mineralization markers *COL10A1* and *ALPL,* we advocate that *TNFRSF11B* affects OA pathophysiology by advancing chondrocyte to osteoblast transition (14). This finding is in line with the observed chondrocalcinosis phenotype observed in previously described members of the family with early-onset OA and carriers of readthrough mutation in *TNFRSF11B* also known as the CCAL1 locus (7).

With *TNFRSF11B* encoding the decoy receptor OPG, which competes for binding of RANKL to the RANK receptor, we next examined expression of *TNFRSF11A* (encoding RANK) and *TNFSF11* (encoding RANKL) upon *TNFRSF11B* upregulation. Even though this triad, and particularly the RANKL/OPG ratio, is known to be an important determinant of bone mass and skeletal integrity (5, 6), no significant changes in *TNFRSF11A* or *TNFSF11* levels were observed (**Figure 4, Supplementary Table S2**). This, together with the fact that we did not find high correlation of expression between *TNFRSF11B* with *TNFRSF11A* or *TNFSF11* in preserved and lesioned OA cartilage, would suggest that in cartilage the interaction among the triad may not play such an important role as in bone. This is in line with the finding of Komuro *et al*. and Tat *et al*. (14, 15), showing no alterations in RANK and OPG expression upon adding exogenous RANKL to chondrocytes.

OPG at high concentration is well known to decrease tumor necrosis factor-related apoptosis-inducing ligand (TRAIL) in chondrocytes, as such inhibiting apoptosis (15, 16).Given that we observed high upregulation of *MMP13* in combination with the upregulation of characteristic osteogenic genes *RUNX2, POSTN, BMP6, ASPN,* and *OGN* (**Figure 4**), which is an opposite response to that of OPG binding to TRAIL (17), we advocate that OPG rather affects OA pathophysiology in cartilage by advancing chondrocyte to osteoblast transition (14). On the other hand, in our spherical neo-cartilage pellets model, we have studied the effect of OPG overexpression at an early timepoint in postmitotic chondrocytes that are stimulated to deposit matrix without further proliferation. As such this model may not be optimal to provide insight into TRAIL-related signaling role of OPG.

In order to determine the co-expression network of OPG signaling in articular cartilage and with OA pathophysiology, we explored a previously assessed RNA sequencing dataset of preserved and lesioned OA cartilage for correlation with *TNFRSF11B* (4). We found 51 genes that highly correlated with *TNFRSF11B* ($r \geq 0.75$), such as *CDH19* (r=0.88) encoding for cadherins involved in calcium-dependent cell-cell adhesion, or *SLC15A3* (r=-0.81) encoding histidine and osteoclast transporters (18). From this network, expression of 30 genes were compared between control and *TNFRSF11B* overexpressing chondrocytes. Despite the high correlations with *TNFRSF11B*, notably only eight genes were found to be responsive to *TNFRSF11B* upregulation (26.6%; *CDON*, *BMP6*, *CDH19*, *P3H2, WNT16, SLC16A7, SLC15A3* and *FITM2)*. This may be explained partly by the fact that genes are upstream of OPG. Alternatively, genes may be correlated to *TNFRSF11B* as a general result of ongoing OA disease processes. Notable among the *TNFRSF11B* correlated and responsive genes were *BMP6* and *SLC15A3* (**Figure 5**). *BMP6* (r=0.77), encoding bone morphogenic protein 6, is well known to be involved in bone formation (19), and *SLC15A3* (r=-0.81) an osteoclast transporter of which lower expression would likely result in a reduction of the number of available osteoclasts. Additionally,

we identified increased expression of *FITM2* (r=0.76) and *SLC16A7* (r=0.77), genes involved in lipid droplet formation and metabolite transport, respectively. Lipid droplets have been reported in OA cartilage (20) and during the osteogenesis process, where osteoprogenitors and osteoblasts synthesize them to use them as energy supplies for the differentiation process (21). More importantly, it has recently been confirmed in mice that fat metabolism is a critical antagonist of cartilage health and integrity (22). Notable as being co-expressed and highly responsive to *TNFRSF11B* was *CDON* (Cell Adhesion Associated, Oncogene Regulated; r=0.83). Although little is known about its direct role in cartilage or bone homeostasis, cadherin signaling is known to be essential for successful cell differentiation, as it has been previously shown for osteogenesis (23, 24). Lastly, expression of *ANKH* (r=0.84), a gene previously associated with chondrocalcinosis and early OA (25, 26), was not affected by *TNFRSF11B* upregulation. This would confirm the work performed in porcine chondrocytes by Williams et al. (6) and translate it to primary human chondrocytes where *ANKH* would affect chondrocalcinosis by a *TNFRSF11B*-independent mechanism.

Remarkably, the study by Zhu et al. (27), showed a different signaling outcome upon overexpression of OPG (CCAL1) in primary human chondrocytes from OA patients. In contrast to results shown here, they observed a fibrotic effect, dominated by reduced expression of *COL2A1* and *SOX9* and a higher expression of *COL1A1*. Several factors may have contributed to this disparity in results. Likely, the most important difference is the use of a 2D model that was previously demonstrated to rather result in a hypertrophic phenotype (28).

Additionally, a previously published trial claimed minimal but debatable effects in OA joints upon treatment with strontium ranelate, a drug licensed for osteoporosis (29, 30). Strontium ranelate increased bone formation while decreasing bone resorption via stimulation of OPG and was thought to target unbeneficial changes in subchondral bone with OA. Considering our current results showing the effect of OPG on cartilage, we advocate that the risk of such an oral treatment to OA patients is seriously underestimated and bound to considerably increase the burden of OA.

A potential limitation of our study is that we have mainly focused on gene expression responses of hPACs by RT-qPCR at day 7 of matrix deposition. Henceforth, due to the early timepoint taken for these analyses and the inherently lower sensitivity and more challenging quantification methods that regular protein analyses such as immunoblotting offer, we have not extensively quantified our changes at a protein level. To further confirm, for example, whether the high upregulation of *MMP13* results in significant changes in protein expression or, for that matter matrix degeneration, later harvesting timepoints (day 14 or day 21) and increasing sample sizes may be required.

In conclusion, we here highlighted the role of *TNFRSF11B* upregulation in OA pathophysiology. Results of our 3D *in vitro* chondrogenesis model indicate that the observed consistent upregulation of *TNFRSF11B* in lesioned OA cartilage may act as a direct driving factor for chondrocyte to osteoblast transition occurring in OA pathophysiology. Moreover, we showed that this transition does not act via the OPG/RANK/RANKL triad, known for that matter in bone remodeling. Together, our results merit further exploration of *TNFRSF11B* as a promising disease OA modifying factor.

Acknowledgements

We thank all the participants of the RAAK study. The LUMC has and is supporting the RAAK study. We thank all the members of our group for valuable discussion and feedback, especially Evelyn Houtman and Ritchie Timmermans. We also thank Enrike van der Linden, Demiën Broekhuis, Peter van Schie, Shaho Hasan, Maartje Meijer, Daisy Latijnhouwers and Geert Spierenburg for collecting the RAAK material. We thank the Sequence Analysis Support Core (SASC) of the Leiden University Medical Center for their support.

Funding

Research leading to these results has received funding from the Dutch Arthritis Society (DAF-16-1-406), and the Dutch Scientific Research council NWO/ZonMW VICI scheme (nr 91816631/528). Data is generated within the scope of the Medical Delta programs Regenerative Medicine 4D ('Generating complex tissues with stem cells and printing technology and Improving Mobility with Technology').

Disclosure of potential conflicts of interest

None declared.

Data availability statement

The data that support the funding of this study are available from the corresponding author upon request.

Ethics approval and consent to participate

The Medical Ethics Committee of the LUMC gave approval for the RAAK study (P08.239). Written informed consent was obtained from all donors.

REFERENCES

1. Chen D, Shen J, Zhao W, Wang T, Han L, Hamilton JL, et al. Osteoarthritis: toward a comprehensive understanding of pathological mechanism. Bone Res. 2017;5:16044.
2. Cucchiarini M, de Girolamo L, Filardo G, Oliveira JM, Orth P, Pape D, et al. Basic science of osteoarthritis. J Exp Orthop. 2016;3(1):22.
3. Dunn SL, Soul J, Anand S, Schwartz JM, Boot-Handford RP, Hardingham TE. Gene expression changes in damaged osteoarthritic cartilage identify a signature of non-chondrogenic and mechanical responses. Osteoarthritis Cartilage. 2016;24(8):1431-40.
4. Coutinho de Almeida R, Ramos YFM, Mahfouz A, den Hollander W, Lakenberg N, Houtman E, et al. RNA sequencing data integration reveals an miRNA interactome of osteoarthritis cartilage. Ann Rheum Dis. 2019;78(2):270-7.
5. Styrkarsdottir U, Lund SH, Thorleifsson G, Zink F, Stefansson OA, Sigurdsson JK, et al. Meta-analysis of Icelandic and UK data sets identifies missense variants in SMO, IL11, COL11A1 and 13 more new loci associated with osteoarthritis. Nat Genet. 2018;50(12):1681-7.
6. Williams CJ, Qazi U, Bernstein M, Charniak A, Gohr C, Mitton-Fitzgerald E, et al. Mutations in osteoprotegerin account for the CCAL1 locus in calcium pyrophosphate deposition disease. Osteoarthritis Cartilage. 2018;26(6):797-806.
7. Ramos YF, Bos SD, van der Breggen R, Kloppenburg M, Ye K, Lameijer EW, et al. A gain of function mutation in *TNFRSF11B* encoding osteoprotegerin causes osteoarthritis with chondrocalcinosis. Ann Rheum Dis. 2015;74(9):1756-62.
8. Pelletier JP, Boileau C, Brunet J, Boily M, Lajeunesse D, Reboul P, et al. The inhibition of subchondral bone resorption in the early phase of experimental dog osteoarthritis by licofelone is associated with a reduction in the synthesis of MMP-13 and cathepsin K. Bone. 2004;34(3):527-38.
9. Cianferotti L, D'Asta F, Brandi ML. A review on strontium ranelate long-term antifracture efficacy in the treatment of postmenopausal osteoporosis. Ther Adv Musculoskelet Dis. 2013;5(3):127-39.
10. Rodrigues TA, Freire AO, Bonfim BF, Cartagenes MSS, Garcia JBS. Strontium ranelate as a possible disease-modifying osteoarthritis drug: a systematic review. Braz J Med Biol Res. 2018;51(8):e7440.
11. Chu JG, Dai MW, Wang Y, Tian FM, Song HP, Xiao YP, et al. Strontium ranelate causes osteophytes overgrowth in a model of early phase osteoarthritis. BMC Musculoskelet Disord. 2017;18(1):78.
12. Bomer N, den Hollander W, Ramos YF, Bos SD, van der Breggen R, Lakenberg N, et al. Underlying molecular mechanisms of DIO2 susceptibility in symptomatic osteoarthritis. Ann Rheum Dis. 2015;74(8):1571-9.
13. Szklarczyk D, Gable AL, Lyon D, Junge A, Wyder S, Huerta-Cepas J, et al. STRING v11: protein-protein association networks with increased coverage, supporting functional discovery in genome-wide experimental datasets. Nucleic Acids Res. 2019;47(D1):D607-D13.
14. Aghajanian P, Mohan S. The art of building bone: emerging role of chondrocyte-to-osteoblast transdifferentiation in endochondral ossification. Bone Res. 2018;6:19.
15. Park DR, Kim J, Kim GM, Lee H, Kim M, Hwang D, et al. Osteoclast-associated receptor blockade prevents articular cartilage destruction via chondrocyte apoptosis regulation. Nat Commun. 2020;11(1):4343.
16. Shimizu S, Asou Y, Itoh S, Chung UI, Kawaguchi H, Shinomiya K, et al. Prevention of cartilage destruction with intraarticular osteoclastogenesis inhibitory factor/osteoprotegerin in a murine model of osteoarthritis. Arthritis Rheum. 2007;56(10):3358-65.
17. Qin X, Jiang Q, Nagano K, Moriishi T, Miyazaki T, Komori H, et al. Runx2 is essential for the transdifferentiation of chondrocytes into osteoblasts. PLoS Genet. 2020;16(11):e1009169.

18. Song F, Yi Y, Li C, Hu Y, Wang J, Smith DE, et al. Regulation and biological role of the peptide/histidine transporter SLC15A3 in Toll-like receptor-mediated inflammatory responses in macrophage. Cell Death Dis. 2018;9(7):770.
19. Wu M, Chen G, Li YP. TGF-beta and BMP signaling in osteoblast, skeletal development, and bone formation, homeostasis and disease. Bone Res. 2016;4:16009.
20. Mansfield JC, Winlove CP. Lipid distribution, composition and uptake in bovine articular cartilage studied using Raman micro-spectrometry and confocal microscopy. J Anat. 2017;231(1):156-66.
21. Rendina-Ruedy E, Guntur AR, Rosen CJ. Intracellular lipid droplets support osteoblast function. Adipocyte. 2017;6(3):250-8.
22. Collins KH, Lenz KL, Pollitt EN, Ferguson D, Hutson I, Springer LE, et al. Adipose tissue is a critical regulator of osteoarthritis. Proc Natl Acad Sci U S A. 2021;118(1).
23. Lee JK, Hu JC, Yamada S, Athanasiou KA. Initiation of Chondrocyte Self-Assembly Requires an Intact Cytoskeletal Network. Tissue Eng Part A. 2016;22(3-4):318-25.
24. Kawaguchi J, Kii I, Sugiyama Y, Takeshita S, Kudo A. The transition of cadherin expression in osteoblast differentiation from mesenchymal cells: consistent expression of cadherin-11 in osteoblast lineage. J Bone Miner Res. 2001;16(2):260-9.
25. Gruber BL, Couto AR, Armas JB, Brown MA, Finzel K, Terkeltaub RA. Novel ANKH amino terminus mutation (Pro5Ser) associated with early-onset calcium pyrophosphate disease with associated phosphaturia. J Clin Rheumatol. 2012;18(4):192-5.
26. Abhishek A, Doherty M. Pathophysiology of articular chondrocalcinosis--role of ANKH. Nat Rev Rheumatol. 2011;7(2):96-104.
27. Zhu H, Yan H, Ma J, Zhang H, Zhang J, Hu Z, et al. CCAL1 enhances osteoarthritis through the NF-kappaB/AMPK signaling pathway. FEBS Open Bio. 2020;10(12):2553-63.
28. Caron MM, Emans PJ, Coolsen MM, Voss L, Surtel DA, Cremers A, et al. Redifferentiation of dedifferentiated human articular chondrocytes: comparison of 2D and 3D cultures. Osteoarthritis Cartilage. 2012;20(10):1170-8.
29. Reginster JY. Efficacy and safety of strontium ranelate in the treatment of knee osteoarthritis: results of a double-blind randomised, placebo-controlled trial. Ann Rheum Dis. 2014;73(2):e8.
30. Lafeber FP, van Laar JM. Strontium ranelate: ready for clinical use as disease-modifying osteoarthritis drug? Ann Rheum Dis. 2013;72(2):157-61.

Supplementary Figures:

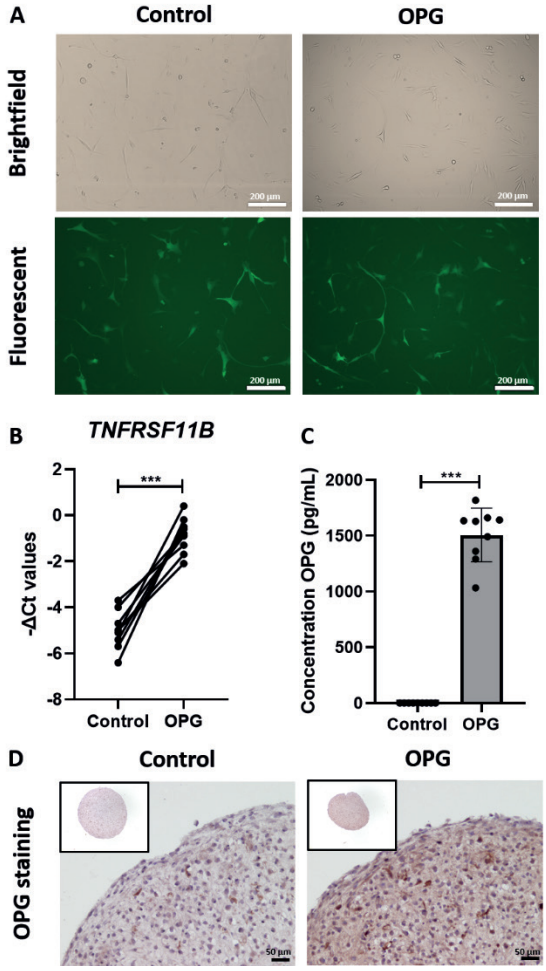

Supplementary Figure S1. Overexpression of *TNFRSF11B* in chondrocytes and quantification of the overexpression by RT-qPCR and ELISA at day 7. A) Representative brightfield and fluorescent images (GFP) of the transduction performed in chondrocytes of the control vector and of the *TNFRSF11B* gene. **B)** RT-qPCR of *TNFRSF11B* in the control samples against *TNFRSF11B* overexpression. **C)** Quantification of OPG (pg/mL) in collected medium measured by ELISA. **D)** OPG staining of the neo-cartilage matrix. Scale bars: 50 µm.

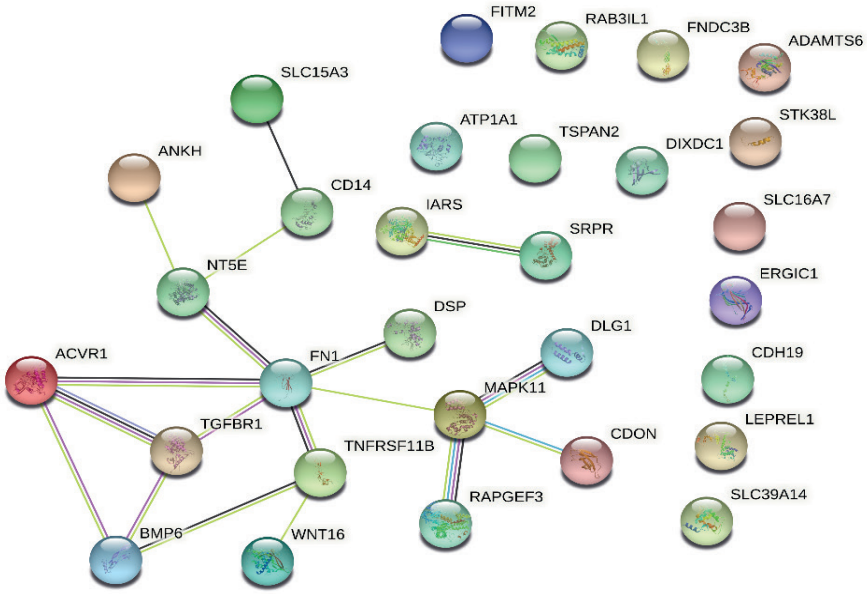

Supplementary Figure S2. Protein-protein interaction network of the 30 selected highly correlated genes to *TNFRSF11B* in STRING. 21 genes with a r≥|0.80|, and 9 genes with a r>|0.75| were added to the online available webtool STRING with a medium confidence interval of 0.4 and a PPI enrichment P-value of $2.11x10^{-6}$.

Supplementary Tables:

Supplementary Table S1. Primer sequences of genes related to cartilage matrix, mineralization and highly correlated to *TNFRSF11B*.

	Primer Sequences	
Matrix Genes	**Fwd**	**Rvs**
ADAMTS5	5′-TGGCTCACGAAATCGGACAT-3′	5′-GCGCTTATCTTCTGTGGAACC-3′
ACAN	5′AGAGACTCACACAGTCGAAACAGC-3′	5′-CTATGTTACAGTGCTCGCCAGTG-3′
ARP	5′-CACCATTGAAATCCTGAGTGATGT-3′	5′-TGACCAGCCGAAAGGAGAAG-3′
COL10A1	5′-GGCAACAGCATTATGACCCA-3′	5′-TGAGATCGATGATGGCACTCC-3′
COL1A1	5′-GTGCTAAAGGTGCCAATGGT-3′	5′-ACCAGGTTCACCGCTGTTAC -3′
COL2A1	5′-CTACCCCAATCCAGCAAACGT-3′	5′-AGGTGATGTTCTGGGAGCCTT-3′
COMP	5′-ACAATGACGGAGTCCCTGAC-3′	5′-TCTGCATCAAAGTCGTCCTG-3′
GAPDH	5′-TGCCATGTAGACCCCTTGAAG-3′	5′-ATGGTACATGACAAGGTGCGG-3′
MMP13	5′-TTGAGCTGGACTCATTGTCG-3′	5′-GGAGCCTCTCAGTCATGGAG-3′
SOX9	5′-CCCCAACAGATCGCCTACAG-3′	5′-CTGGAGTTCTGGTGGTCGGT-3′
Mineralization genes	**Fwd**	**Rvs**
ALPL	5′-CAAAGGCTTCTTCTTGCTGGTG-3′	5′-CCTGCTTGGCTTTTCCTTCA-3′
ASPN	5′-ACACGTTTTGGAAATGAGTGC-3′	5′-GAACACCGTCACCCCTTCAA-3′
OGN	5′-TGATGAAATGCCCACGTGTC-3′	5′-TTTGGTAAGGGTGGTACAGCA-3′
POSTN	5′-TACACTTTGCTGGCACCTGT-3′	5′-TTTAAGGAGGCGCTGATCCA-3′
RUNX2	5′-CAATTTCCTCCTTGCCCCTCA-3′	5′-TCGGATCTACGGGAATACGCA-3′
SPP1	5′-GCCAGTTGCAGCCTTCTCA-3′	5′-AAAAGCAAATCACTGCAATTCTCA-3′
TNFRSF11A	5′-GAAGCTCAGCCTTTTGCTCA-3′	5′-GGGAACCAGATGGGATGTCG-3′
TNFRSF11B	5′-TTGATGGAAAGCTTACCGGGA-3′	5′-TCTGGTCACTGGGTTTGCATG-3′
TNFSF11	5′-CAACAAGGACACAGTGTGCAA-3′	5′-AGGTACAGTTGGTCCAGGGT-3′
***TNFRSF11B*-correlated genes**	**Fwd**	**Rvs**
ACVR1	AGGGCTCATCACCACCAATG	GTAATCTGGCGAGCCACTGT
ADAMTS6	5′-GGTGCAGATACCAAGAGGCT-3′	5′-GCCAGTCAATAGTCCAGGCA-3′
ANKH	5′-GTCTGCATGGCTCTGTCACT-3′	5′-AGGCAAAGTCCACTCCGATG-3′
ATP1A1	5′-TGTACCTGGGTGTGGTGCTA-3′	5′-ATCACAAGGGCTTGCTGAGG-3′
BMP6	5′-GCGGACATGGTCATGAGCTT-3′	5′-ACCTCACCCTCAGGAATCTG-3′
CD14	5′-AGCCACAGGACTTGCACTTT-3′	5′-TGCTTGGGCAATGCTCAGTA-3′
CDH19	5′-TGAGCACCAGAACCACTACG-3′	5′-AAGTGGTGGAAGCCTCAGTG-3′
CDON	5′-ACACCACTCTCTCAGGAGCA-3′	5′-AAGGTGGGAATAGCCACTGC-3′
DIXDC1	5′-CCCAGTCAGAAGAGAAGGCA-3′	5′-GCCGCCAGTCTCGAGATAAT-3′
DLG1	5′-TCTTCCCTCTCCTCCCACTG-3′	5′-GTACTGGGGGAGGATTTGCC-3′

***TNFRSF11B*-correlated genes**	**Fwd**	**Rvs**
DSP	5′-ATGTACTATTCTCGGCGCGG-3′	5′-GTGTTCTGGTTCTGGTGCCT-3′
ERGIC1	5′-TCTGCTGCTGCCTCTTCATC-3′	5′-CCTTGTCTGGGTCATCGACA-3′
FITM2	5′-ACTGATCACTCTGCTGTGGC-3′	5′-GCCATCAGAGGGAGGCATTT-3′
FN1	5′-CCGACCAGAAGTTTGGGTTC-3′	5′-CACGACCATTCCCAACACAC-3′
FNDC3B	5′-CCTGGAACCGTGTATCGCTT-3′	5′-GGTGCTTTGCATTGTCCAGG-3′
HLA-E	5′-GGCCTGGTTCTCCTTGGATC-3′	5′-GCTCCCTCCTTTTCCACCTG-3′
IARS	5′-GGTTGTCCACCAAGCTCCTT-3′	5′-GTTGTGAAGCAGCCTGAAGC-3′
MAPK11	5′-GCCGACCTGAACAACATCGT-3′	5′-TTCAGGTCCCGGTGGATGAT-3′
NT5E	5′-ATTGCACTGGGACATTCGGG-3′	5′-TGGAAGGTGGATTGCCTGTG-3′
P3H2	5′-AGAGAAGCCAAGCCACACAT-3′	5′-GCTTGTTCGAAGTGCCTGAT-3′
RAB3IL1	5′-CAGGAGCGTTGTCTGGAACA-3′	5′-CCAGTGGGTGCAGATTCAGA-3′
RAPGEF3	5′-TCCAGTGCTCATGACCCAAC-3′	5′-ATGGAAGTGGTGCAGAAGGG-3′
SLC15A3	5′-AGGACATCGCCAACTTCCAG-3′	5′-AGACCCTGCAGGACATAGGT-3′
SLC16A7	5′-GGACTCTTGGTGCCAACAGA-3	5′-ACCACAATCCAACCCCATCC-3′
SLC39A14	5′-GAAGGCCCTACTCAACCACC-3′	5′-GTGGGCAGTGAAGAGGTCTC-3′
SRPRA	5′-GGCGTTAATGGAGTGGGGAA-3′	5′-TCACAGGCAGCAATGAGGAC-3′
STK38L	5′-TGAAGAGAGAGAAACCAGGCAG-3′	5′-TTCTTTGCGAGCGTGTTGTG-3′
TGFBR1	5′-TGCAGACTTAGGACTGGCAG-3′	5′-GAGAACTTCAGGGGCCATGT-3′
TSPAN2	5′-CAGGGGAAAAGGCAATGGGA-3′	5′-GCTCCTTTGGGCATGTAGGT-3′
WNT16	5′-AACACCACGGGCAAAGAAAAC-3′	5′-ATCAACTTGGCGACAGCCT-3′

Supplementary table S2. Cartilage health and mineralization gene changes measured by RT-qPCR upon lentiviral induced overexpression of *TNFRSF11B* in a 3D *in vitro* chondrogenesis model. Significant data are highlighted in bold.

Cartilage health			**Mineralization**		
Genes	**FD**	**P value**	**Genes**	**FD**	**P value**
ACAN	1.21	$2.7x10^{-1}$	*ALPL*	4.22	$7.2x10^{-2}$
ADAMTS5	1.03	$3.0x10^{-1}$	***ASPN***	**2.61**	$\mathbf{1.0x10^{-2}}$
COL10A1	4.24	$6.3x10^{-1}$	***OGN***	**1.68**	$\mathbf{2.3x10^{-2}}$
COL1A1	**1.88**	$\mathbf{1.3x10^{-2}}$	***POSTN***	**1.75**	$\mathbf{4.0x10^{-2}}$
COL2A1	**4.77**	$\mathbf{4.8x10^{-4}}$	***RUNX2***	**4.51**	$\mathbf{4.0x10^{-3}}$
COMP	**0.69**	$\mathbf{2.0x10^{-2}}$	*SPP1*	1.94	$1.6x10^{-1}$
MMP13	**14.76**	$\mathbf{2.0x10^{-3}}$	*TNFRSF11A*	2.45	$7.8x10^{-1}$
SOX9	1.02	$4.3x10^{-1}$	*TNFSF11*	1.06	$3.9x10^{-1}$

Supplementary table S3. 51 *TNFRSF11B*-correlated genes from RNA-seq data with an r-value higher than 0.75.

Genes highly correlated to *TNFRSF11B*			
R-value	**Gene**	**R-value**	**Gene**
0.88	*CDH19*	-0.78	*PARP10*
0.87	*ATP1A1*	0.78	*ADGRG2*
0.85	*DIXDC1*	-0.78	*CD14*
0.85	*FN1*	-0.77	*SNCG*
0.84	*STK38L*	0.77	*GLP2R*
0.84	*ANKH*	0.77	*R3HDML*
0.84	*TGFBR1*	0.77	*SLC16A7*
0.83	*CDON*	0.77	*BMP6*
0.82	*NT5E*	0.76	*CDK2AP1*
-0.81	*SLC15A3*	0.76	*PAPSS2*
0.81	*ERGIC1*	-0.76	*RAPGEF3*
0.81	*ADAMTS6*	0.76	*CDH10*
0.81	*DSP*	0.76	*IARS*
-0.81	*MAPK11*	0.76	*SLC7A1*
0.80	*SLC39A14*	0.76	*CD109*
0.80	*TSPAN2*	0.76	*PGM2L1*
0.80	*DLG1*	0.76	*TES*
-0.80	*HLA.E*	0.76	*FITM2*
0.80	*SRPRA*	0.76	*CLVS2*
0.79	*P3H2*	-0.76	*FLOT2*
-0.79	*RAB3IL1*	0.75	*ACVR1*
0.79	*DSG2*	0.75	*PPP4R4*
0.79	*TMCO3*	0.75	*GALNT7*
0.79	*SLC1A1*	0.75	*RCAN3*
0.78	*RFTN2*	0.75	*WNT16*
0.78	*FNDC3B*		

Supplementary table S4. Genes highly correlated to *TNFRSF11B* analyzed by RT-qPCR upon lentiviral induced overexpression of *TNFRSF11B* in a 3D *in vitro* chondrogenesis model. Significant data are highlighted in bold.

Expression of genes highly correlated to *TNFRSF11B*					
Genes	**FD**	**P value**	**Genes**	**FD**	**P value**
CDH19	**1.53**	**$4.5x10^{-2}$**	*TSPAN2*	1.23	$1.5x10^{-1}$
ATP1A1	1.01	$6.3x10^{-1}$	*DLG1*	1.06	$6.8x10^{-1}$
DIXDC1	1.13	$7.7x10^{-1}$	*HLA.E*	1.04	$9.0x10^{-1}$
FN1	1.34	$3.0x10^{-1}$	*SRPRA*	1.27	$2.3x10^{-1}$
STK38L	1.23	$3.6x10^{-1}$	***P3H2***	**1.48**	**$4.7x10^{-2}$**
ANKH	1.34	$1.8x10^{-1}$	*RAB3IL1*	1.30	$9.5x10^{-1}$
TGFBR1	1.10	$8.6x10^{-1}$	***BMP6***	**9.34**	**$2.6x10^{-2}$**
CDON	**2.03**	**$5.0x10^{-3}$**	***WNT16***	**0.81**	**$4.3x10^{-2}$**
NT5E	1.29	$2.5x10^{-1}$	*ACVR1*	1.31	$5.5x10^{-1}$
SLC15A3	**0.40**	**$4.0x10^{-3}$**	*FNDC3B*	1.19	$3.0x10^{-1}$
ERGIC1	1.12	$4.7x10^{-1}$	*CD14*	1.38	$4.8x10^{-1}$
ADAMTS6	1.20	$5.4x10^{-1}$	***SLC16A7***	**1.97**	**$1.8x10^{-2}$**
DSP	0.92	$1.8x10^{-1}$	*RAPGEF3*	1.36	$6.6x10^{-1}$
MAPK11	1.94	$4.5x10^{-1}$	*IARS*	1.26	$1.1x10^{-1}$
SLC39A14	1.03	$9.6x10^{-1}$	***FITM2***	**2.28**	**$1.4x10^{-2}$**